Blending and foaming thermoplastic starch with poly (lactic acid) by CO 2 -aided hot melt extrusion

Margot Chauvet, Martial Sauceau, Fabien Baillon, Jacques Fages

Blending and foaming thermoplastic starch with poly (lactic acid) by CO_2-aided hot melt extrusion

Margot Chauvet | **Martial Sauceau** | **Fabien Baillon** | **Jacques Fages**

IMT Mines Albi; CNRS; Centre RAPSODEE, Université de Toulouse, Albi, France

Correspondence
Jacques Fages, IMT Mines Albi; CNRS; Centre RAPSODEE, Université de Toulouse, F- 81013 Albi, France.
Email: jacques.fages@mines-albi.fr

Abstract

Biomaterials are materials that can be biodegradable or obtained from renewable resources. Among them, poly (lactic acid) (PLA) and thermoplastic starch (TPS) represent an interesting alternative to replace petro-sourced thermoplastics. In this study, blends made by TPS addition to PLA were subjected to a foaming process using supercritical CO_2-aided extrusion. Extruder die temperature and CO_2 content were the most prominent parameters explaining the structure of the foams obtained. Both parameters were intimately linked since the CO_2 flow depends on the melt temperature, the lower the temperature, the higher the CO_2 solubility. Therefore, the die temperature was chosen to pilot the process. Whatever the experimental conditions, a 50/50 (in wt%) blend was poorly foamed due to the strong incompatibility between both biopolymers. However, the blend made of 80 wt% PLA and 20 wt% TPS gave evenly foamed samples. In terms of expansion and type of porosity this blend behaved like pure PLA with high porosity, up to 96%, and the presence of a threshold die temperature separating a close cell porosity at lowest temperatures and an open cell structure above the threshold. This temperature threshold was however significantly lower to that obtained with pure PLA.

KEYWORDS

biopolymers, extrusion, foams, supercritical CO_2

1 | INTRODUCTION

There is a strong rise both in the general public's and the scientific community's awareness linked to the massive use of polymeric materials. They are mainly obtained from petroleum resources, and besides their questionable ability to be recycled, they are often non-degradable and a lot of waste is dumped in the environment.[1] As a consequence, pollution of soils and oceans by these wastes are becoming a major environmental issue. Therefore, biopolymers can be regarded as an interesting alternative.[2] They are materials that can be biodegradable and/or obtained from renewable resources. For instance, the poly(lactic acid) (PLA) is produced by polymerization of lactic acid, which is obtained by the fermentation of simple sugars coming from enzymatic hydrolysis of vegetal polysaccharides such as starch.[3,4] Moreover, PLA also responds to the definition of biopolymer because it is degraded by hydrolysis, after several months of exposure to moisture, and it presents biocompatible properties for medical applications. Starch is stored in cereal grains such as barley, oats, wheat, rice, and corn or in underground tubers, as it is the case with potatoes, cassava and yam. It is totally biodegradable in a wide variety of environments. It can be hydrolysed into glucose by microorganism or enzymes, and then metabolized into carbon dioxide and water.[5] When starch is exposed to shear and high temperature (>100°C) in the presence of a

plasticizer (e.g., water, glycerol or sorbitol), it behaves like a thermoplastic.[6] In this case, the plasticizer will break the intermolecular and intramolecular hydrogen bonds, thus destroying the granular structure of the starch. Thermoplastic starch (TPS) present two main features: it exhibits a strong hydrophilic character and low mechanical properties. To reduce these shortcomings, TPS is often blended with other biopolymers.

Foams of PLA or its composites may have applications in many industrial fields including biomedicine as controlled drug delivery systems or scaffolds in implant for living tissues.[7,8] Our group studied the process of hot extrusion assisted by supercritical CO_2 to optimize the foaming of several polymers.[9–11] In a previous publication,[12] we explored the influence of the die temperature and the addition of a static mixer on the properties of PLA foams. The most significant result was the demonstration of the presence of a threshold die temperature, on both sides of which the properties of the foams were very different. Above this temperature threshold of 109°C, samples of low crystallinity were obtained due to the preponderance of thermal agitation over the shear effects and the plasticization effects of dissolved CO_2, resulting in low elongational viscosity. As a result, large radial expansion was induced and samples of extrudate up to 18 mm in diameter were obtained by using a cylindrical die of 3 mm diameter. These samples had open porosity, with a total porosity of up to 96%. On the other hand, below the temperature threshold, the crystallinity of the sample increased, which resulted in a high melt strength. This low die temperature caused a "freezing" of the surface with the consequence of an induced longitudinal expansion to compensate for the absence of radial expansion. In this case, the foams displayed a closed cell morphology because the CO_2 could not escape through the cell walls. However, the total porosity remained high (>92%).

Literature has shown the interest of blending these two polymers. Historically, starch was added to PLA to decrease the PLA price and to improve the biodegradation properties.[13,14] Since PLA is hydrophobic and starch is hydrophilic, there may be compatibility issues due to low interfacial interactions. However, given that starch is gelatinized or plasticized, thus disintegrating granules and overcoming the strong interaction of starch molecules in the presence of water and other plasticizers, its dispersion in other polymers will be improved.[15] Several authors have shown that adding a third component with a compatibilizing effect, will improve the interfacial bonding between two polymers.[16–20]

In this article, we have investigated the behavior of PLA/TPS foams obtained by the same process of CO_2-assisted hot-melt extrusion. Two different blends of PLA and TPS have been studied: 80 wt% PLA with 20 wt% TPS and 50 wt% PLA with 50 wt% TPS. In the first blend, the PLA was preponderant, and we wanted to establish whether it behaved like pure PLA. In the other blend, both polymers were present in equal quantity. The objectives were the elucidation of the effects of CO_2 content in the polymer melt as well as the influence of the die temperature on the morphology of the foams thus manufactured.

2 | EXPERIMENTAL

2.1 | Materials

The PLA used is commercial grade (PLE001, NaturePlast, France) with a semi-crystalline nature and a Melt Flow Index (MFI) of 6 g/10 min (210°C, 2.16 kg). Its density, measured by water pycnometry, is equal to 1230.9 kg/m^3. DSC cycle has shown a glass transition at 59°C and the melting temperature is approximately 150°C.

The TPS used is the grade NPWS001 from NaturePlast. It presents good permeability to water vapor, as well as barrier properties to oxygen and carbon dioxide.

Carbon dioxide (CO_2) with a purity of 99.995%, was supplied by Air Liquide (France).

2.2 | Masterbatch preparation

Two blends containing 80 wt% PLA + 20 wt% TPS (named 80PLA/20TPS), and 50 wt% PLA + 50 wt% TPS (named 50PLA/50TPS) were prepared on a co-rotating twin screw extruder BC12 (Clextral) with a length of 900 mm and a diameter of 25 mm (ratio L/D of 36). For the blend of 80PLA/20TPS, the temperatures of the 12 parts were kept in the range 60–190°C, for the other blend the temperatures were between 60 and 180°C.

2.3 | Extrusion foaming

Experiment of extrusion foaming was performed on a single-screw extruder. A schematic representation of this equipment is shown in Figure 1. The single-screw extruder has a 30 mm screw diameter and a length to diameter ratio (L/D) of 37 (Rheoscam, Scamex). This experimental set-up has been described in details in a previous publication.[12] The screw can turn at a rotation speed N from 30 to 80 rpm. At the end of the extruder, a removable part is added to enhance both distributive and dispersive mixing and to improve the sorption and dissolution of the CO_2 in the polymer melt. It contains four static mixer elements with a diameter of 17 mm (SMB-H 17/4, Sulzer). After the static mixer, a cylindrical die of 3 mm diameter and 12 mm length is installed. The

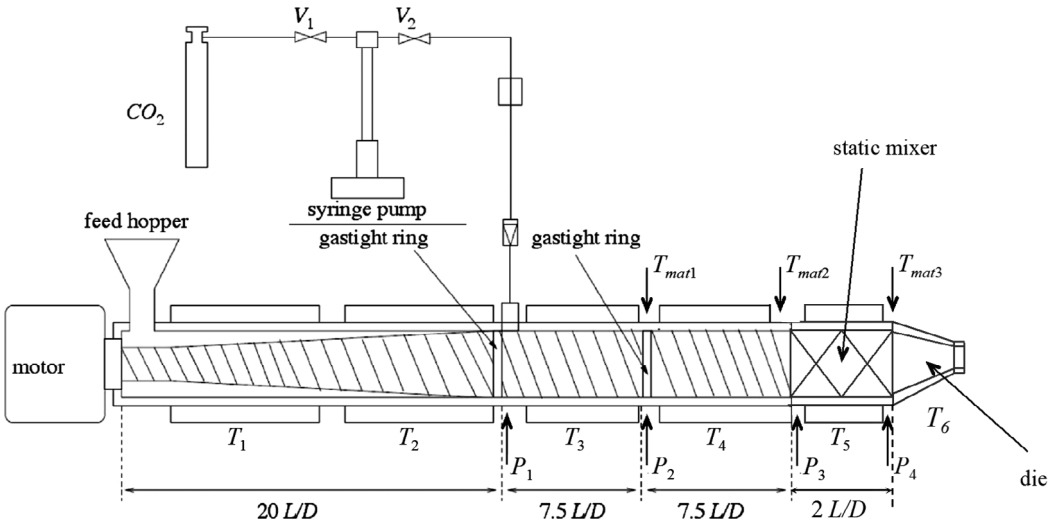

FIGURE 1 The single-screw extruder used with its CO_2 injection device

TABLE 1 Operating conditions of extrusion foaming experiments

	100TPS	80PLA/20TPS	50PLA/50TPS
T_1 (°C)	50	140	120
T_2 (°C)	150	165	145
T_3 (°C)	150	165	145
T_4 (°C)	130	145	135
T_5 (°C)	86–105	86–140	95–140
T_6 (°C)	$=T_5$	$=T_5$	$=T_5$
$\dot{V}_{CO_2}$ (ml/min)	1–2	1.5–4.5	1.5–3
N (rpm)	40	30	30

temperature inside the barrel is regulated at six locations: T_1 and T_2 before the CO_2 injection, T_3 and T_4 after the injection, T_5 in the static mixer and T_6 in the die. There are four pressure and three temperature sensors: P_1 after the CO_2 injector, P_2 and T_{mat1} before the second gastight ring, P_3 and T_{mat2} before the static mixer and P_4 and T_{mat3} by the die. Carbon dioxide, pumped from a cylinder by a syringe pump (260D, ISCO), is injected in the extruder barrel at a length to diameter ratio of 20 from the feed hopper at the same pressure as that of the extruder. The pump runs in a constant volumetric flow rate mode ($\dot{V}_{CO_2}$). The mass flow rate of polymer $\dot{m}^m_{polymer}$ is measured at the die exit by collecting and weighing a sample taken on a period of time. The mass fraction of CO_2 (w_{CO2}) can be then calculated by using the CO_2 density in the pump $\rho^{pump}_{CO_2}$ (at 5°C and P_1) obtained on NIST website and calculated by the Span and Wagner equation of state.[12,21]

Some operating conditions (T_1-T_4) were kept constant and depend on the composition, while T_5, T_6 and $\dot{V}_{CO_2}$ have been varied. Table 1 shows the different operating conditions applied while Tables 2–4 list the samples collected for TPS, 80PLA/20TPS and 50PLA/50TPS blends respectively.

Samples are in the shape of cylindrical rod, the dimensions of which depend on both the total porosity and the type of porosity. The diameter can be calculated from the radial expansion which is defined as the ratio of this diameter to that of the die (3 mm).

2.4 | Foam characterizations

All the characterizations have been carried out on three different samples to calculate the average and the standard deviation, or at least to check the repeatability (SEM pictures).

2.4.1 | Morphology

The samples were observed by environmental scanning electron microscopy (TM3030 Plus, MiniMEB, Hitachi). Pictures were taken on cross sections perpendicular to the axis of the rod extrudate, using secondary electrons signal with a low accelerating voltage of 5 keV, which allows direct observation without any sample metal coating.

2.4.2 | Porosity

The foam porosity (ε_T), representing the ratio of void volume to the total volume of the sample, can be calculated by the following Equation (1):

$$\varepsilon_T = \frac{V_{Total\ porosity}}{V_{Total}} = 1 - \frac{\rho_f^{H_2O}}{\rho_p^{H_2O}}, \quad (1)$$

With: $\rho_f^{H_2O}$ the apparent density of the foamed sample, determined by water pycnometry; $\rho_p^{H_2O}$ the solid polymer density, determined by helium pycnometry (AccuPYC 1330, Micromeretics).

The open porosity (ε_O), representing the ratio of open cell to the total volume of the sample can be calculated by the following Equation (2):

$$\varepsilon_O = \frac{V_{Open\ porosity}}{V_{Total}} = 1 - \frac{\rho_f^{H_2O}}{\rho_f^{He}}, \quad (2)$$

With: ρ_f^{He} the density of the foamed sample excluding open pores determined by helium pycnometry.

The open-cell content (OC), representing the ratio of open porosity to the total porosity, can be calculated by the following Equation (3):

$$OC = \frac{\varepsilon_O}{\varepsilon_T}. \quad (3)$$

TABLE 2 Samples collected for TPS

Sample name	T_6 (°C)	$\dot{V}_{CO_2}$ (ml/min)	$\dot{m}^m_{polymer}$ (g/min)	P_1 (MPa)	$\rho^{pump}_{CO_2}$ (g/ml)	w_{CO_2} (%)
TPS_105_0	105	0	36.9	1.0	0.9175	0
TPS_105_1	105	1	30.3	10.0	0.9566	3.1
TPS_101_1	101	1	32.8	10.6	0.9562	2.8
TPS_96_1	96	1	28.5	11.3	0.9623	3.3
TPS_91_1.5	91	1.5	32.2	12.7	0.9684	4.3
TPS_86_2	86	2	25.8	11.4	0.9627	6.9

TABLE 3 Samples collected for blend of PLA (80%) and TPS (20%)

Sample name	T_6 (°C)	$\dot{V}_{CO_2}$ (ml/min)	$\dot{m}^m_{polymer}$ (g/min)	P_1 (MPa)	$\rho^{pump}_{CO_2}$ (g/ml)	w_{CO_2} (%)	χ (%)
80PLA/20TPS_140_0	140	0	46.1	14.7	0.9770	0	5.0
80PLA/20TPS_135_0	135	0	45.1	15.3	0.9797	0	
80PLA/20TPS_130_0	130	0	45.24	16.6	0.9853	0	
80PLA/20TPS_130_1.5	130	1.5	43.6	14.9	0.9779	3.3	1.7
80PLA/20TPS_123_1.5	123	1.5	44.24	14.9	0.9779	3.2	
80PLA/20TPS_120_1.5	120	1.5	44.14	15.5	0.9805	3.2	1.9
80PLA/20TPS_120_2	120	2	44.46	15.9	0.9823	4.2	
80PLA/20TPS_114_2	114	2	44.54	16.6	0.9853	4.2	
80PLA/20TPS_112_2.5	112	2.5	45.9	17.3	0.9883	5.1	6.0
80PLA/20TPS_109_2.5	109	2.5	46.62	17.3	0.9883	5.0	
80PLA/20TPS_106_3	106	3	45.26	17.8	0.9905	6.2	
80PLA/20TPS_104_3	104	3	45.26	18.3	0.9927	6.2	4.8
80PLA/20TPS_102_3.5	102	3.5	45.02	18.8	0.9949	7.2	
80PLA/20TPS_100_3.5	100	3.5	43.46	19.5	0.9979	7.4	
80PLA/20TPS_99_4	99	4	43.18	19.9	0.9996	8.5	7.0
80PLA/20TPS_95_4	95	4	44.1	20.8	1.0036	8.3	5.4
80PLA/20TPS_92_4.5	92	4.5	42.22	21.4	1.0062	9.7	11.2
80PLA/20TPS_90_4.5	90	4.5	48.88	21.4	1.0062	8.5	
80PLA/20TPS_89_4.5	89	4.5	41.34	23.1	1.0136	9.9	11.8
80PLA/20TPS_86_4.5	86	4.5	37.56	24.2	1.0183	10.9	11.7

2.4.3 | Expansion

The total expansion (E_T) can be expressed on the basis of the porosity with the following Equation (4):

$$E_T = \frac{\rho_p^{H_2O}}{\rho_f^{H_2O}} = \frac{1}{1-\varepsilon_T}, \quad (4)$$

The total expansion provides the same type of information as porosity but with a special emphasis on high porosity range.

Depending on the CO_2 content, the maximum expansion ratio (E_T^M) can be calculated[22] with the following Equation (5):

TABLE 4 Samples collected for blend of PLA (50%) and TPS (50%)

Sample name	T_6 (°C)	$\dot{V}_{CO_2}$ (ml/min)	$\dot{m}^m_{polymer}$ (g/min)	P_1 (MPa)	$\rho^{pump}_{CO_2}$ (g/ml)	w_{CO_2} (%)	χ (%)
50PLA/50TPS_140_0	140	0	52.64	7	0.9436	0	10.7
50PLA/50TPS_130_0	130	0	55.28	7.1	0.9440	0	
50PLA/50TPS_125_0	125	0	53.5	11.8	0.9644	0	
50PLA/50TPS_124_1.5	124	1.5	51.46	11.3	0.9623	2.7	2.8
50PLA/50TPS_120_1.5	120	1.5	54	11	0.9610	2.6	
50PLA/50TPS_115_1.5	115	1.5	51.1	12	0.9653	2.8	7.4
50PLA/50TPS_110_2	110	2	51.2	12.9	0.9692	3.7	
50PLA/50TPS_105_2	105	2	51.24	13.9	0.9736	3.7	15.7
50PLA/50TPS_101_2.5	101	2.5	50.1	15.3	0.9797	4.7	
50PLA/50TPS_98_2.5	98	2.5	52.9	17.2	0.9879	4.5	12.7
50PLA/50TPS_96_3	96	3	46.96	17	0.9870	5.9	8.7
50PLA/50TPS_95_3	95	3	47.28	19.8	0.9992	6	

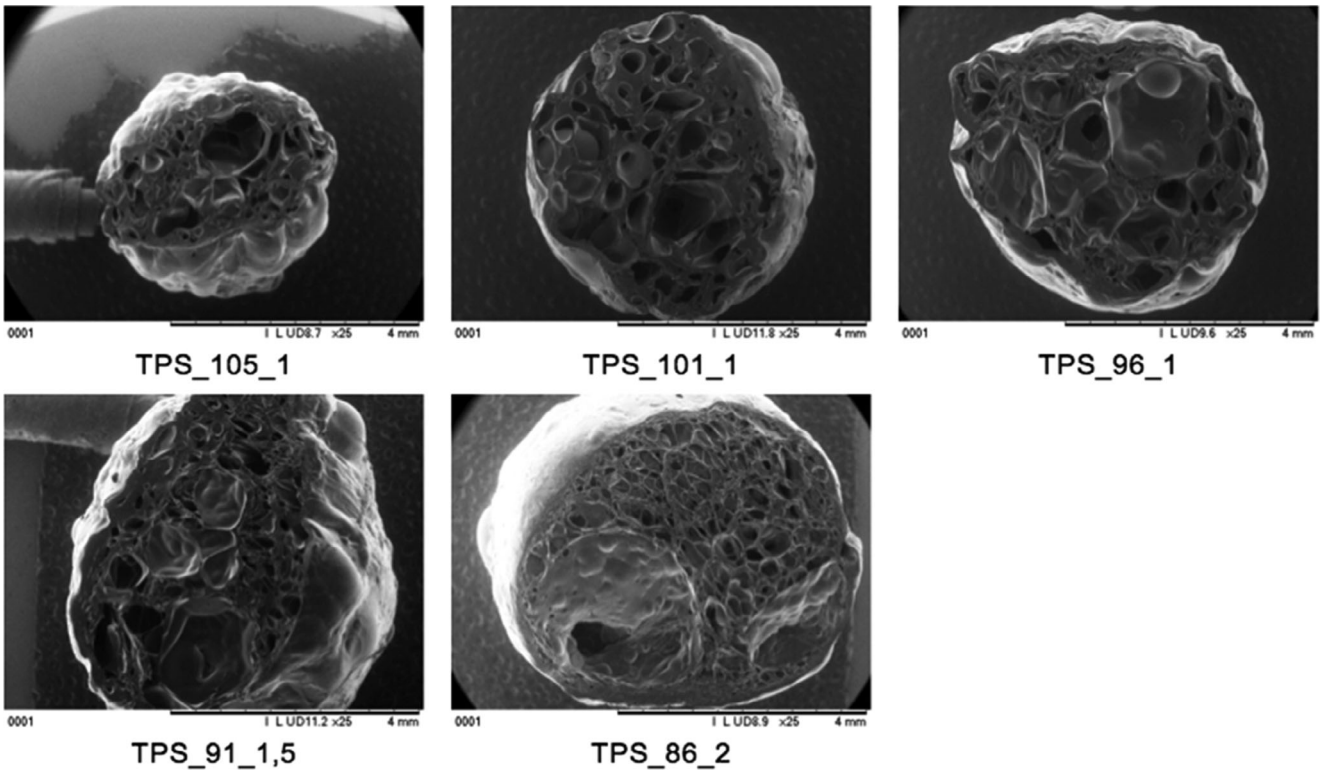

FIGURE 2 SEM microphotographs of TPS foams extruded at different die temperatures

$$E_T^M = \frac{V_{polymer} + V_{CO_2}^{amb}}{V_{polymer}} = 1 + \frac{w_{CO_2}}{1 - w_{CO_2}} \times \frac{\rho_p^{H_2O}}{\rho_{CO_2}^{amb}}, \quad (5)$$

With: w_{CO2} the mass fraction of CO_2; $\rho_p^{H_2O}$ the solid polymer density; $\rho_{CO_2}^{amb}$ the CO_2 density at room pressure and temperature. The value of this last parameter is obtained from the NIST data base: $\rho_{CO_2}^{amb} = 1.78\,kg/m^3$.[21]

The E_T^M calculation is made with the assumption of no CO_2 escape from the sample.[23]

The expansion efficiency (R_E) is the total expansion ratio (E_T) divided by the maximal theoretical expansion ratio (E_T^M). This expansion efficiency gives information about the exact quantity of CO_2 used to expand the foams.

The radial expansion (E_R) was calculated by dividing the diameter of the sample measured with a caliper (average of 10 measurements) by the die diameter (3 mm).

The longitudinal expansion (E_L) was quantified by measuring the sample length exiting the extruder in a period of 30 seconds with and without CO_2, E_L being the ratio of the two.

2.4.4 | Thermal analysis

Modulated Differential Scanning Calorimetry (MDSC, Q2000, TA Instruments) was performed to evaluate the thermal properties and the crystallinity of the foams. All samples were placed in a non hermetic aluminium pan

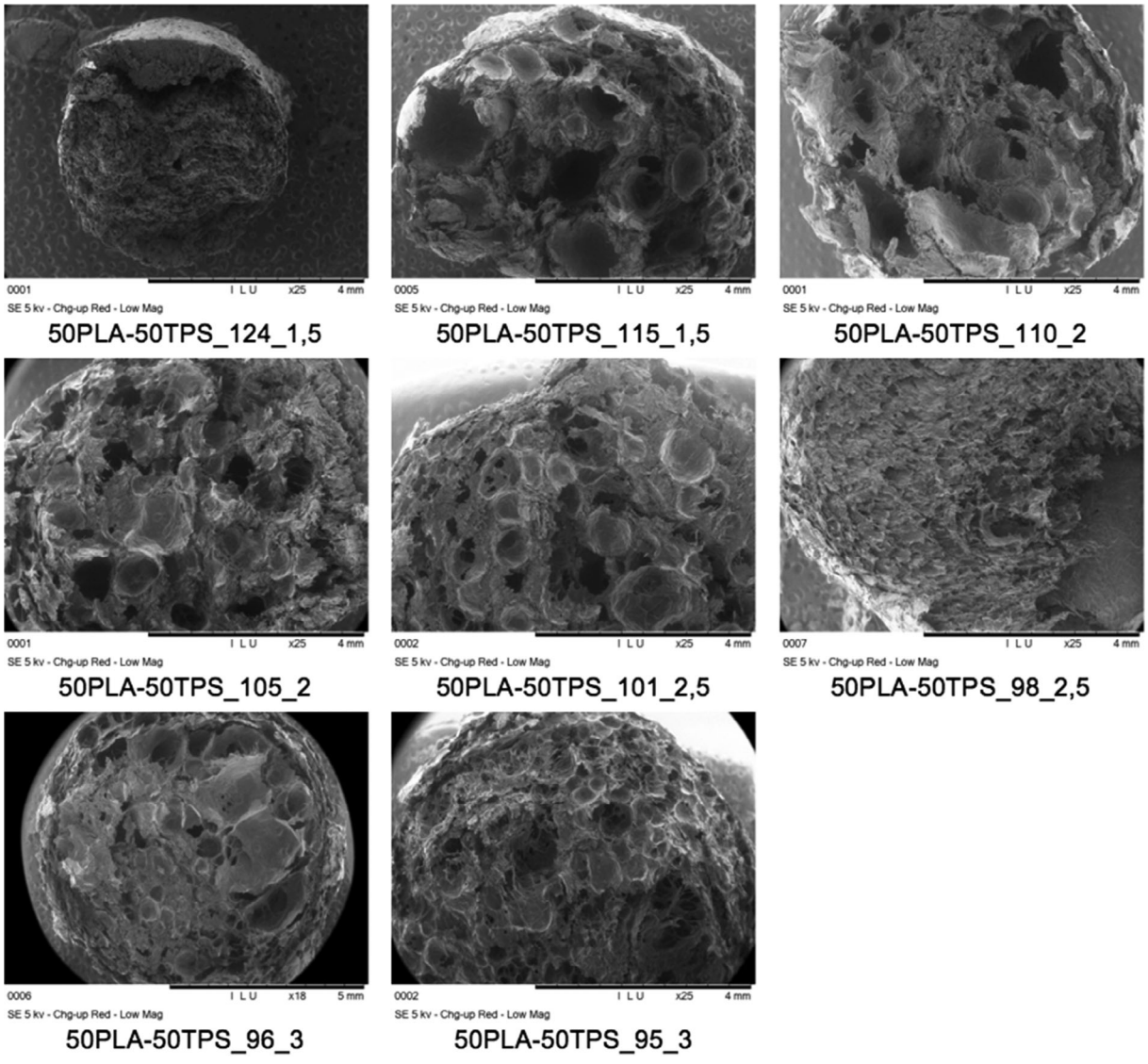

FIGURE 3 SEM microphotographs of 50PLA/50TPS foams at different die temperatures

with a nitrogen sweeping. The analyses were performed on Heat Only mode, from −80 to 200°C with a heating ramp of 2°C/min. An amplitude of 0.32°C was applied with a time period of 60 s.

The crystallinity χ of the sample is calculated with the following Equation (6):

$$\chi = \frac{\Delta H_m - \Delta H_{cc}}{\Delta H_{m\infty}}, \quad (6)$$

with ΔH_m the melting enthalpy, ΔH_{cc} the cold crystallization enthalpy and $\Delta H_{m\infty}$ the heat of fusion of PLA for a perfect crystal, known to be 93 J/g.[24]

3 | RESULTS AND DISCUSSION

3.1 | Morphological characterization of the foams by SEM analysis

3.1.1 | Pure TPS

As shown in Figure 2, at high temperature, TPS foam structure was inhomogeneous with pore of different size and no spherical shape. With temperature diminution, the cell density increased with a reduction of cell size. However even at low temperature, cell size distribution was quite broad. It was hypothesized that cells have nucleated and have been broken due to the amorphous character of the starch.

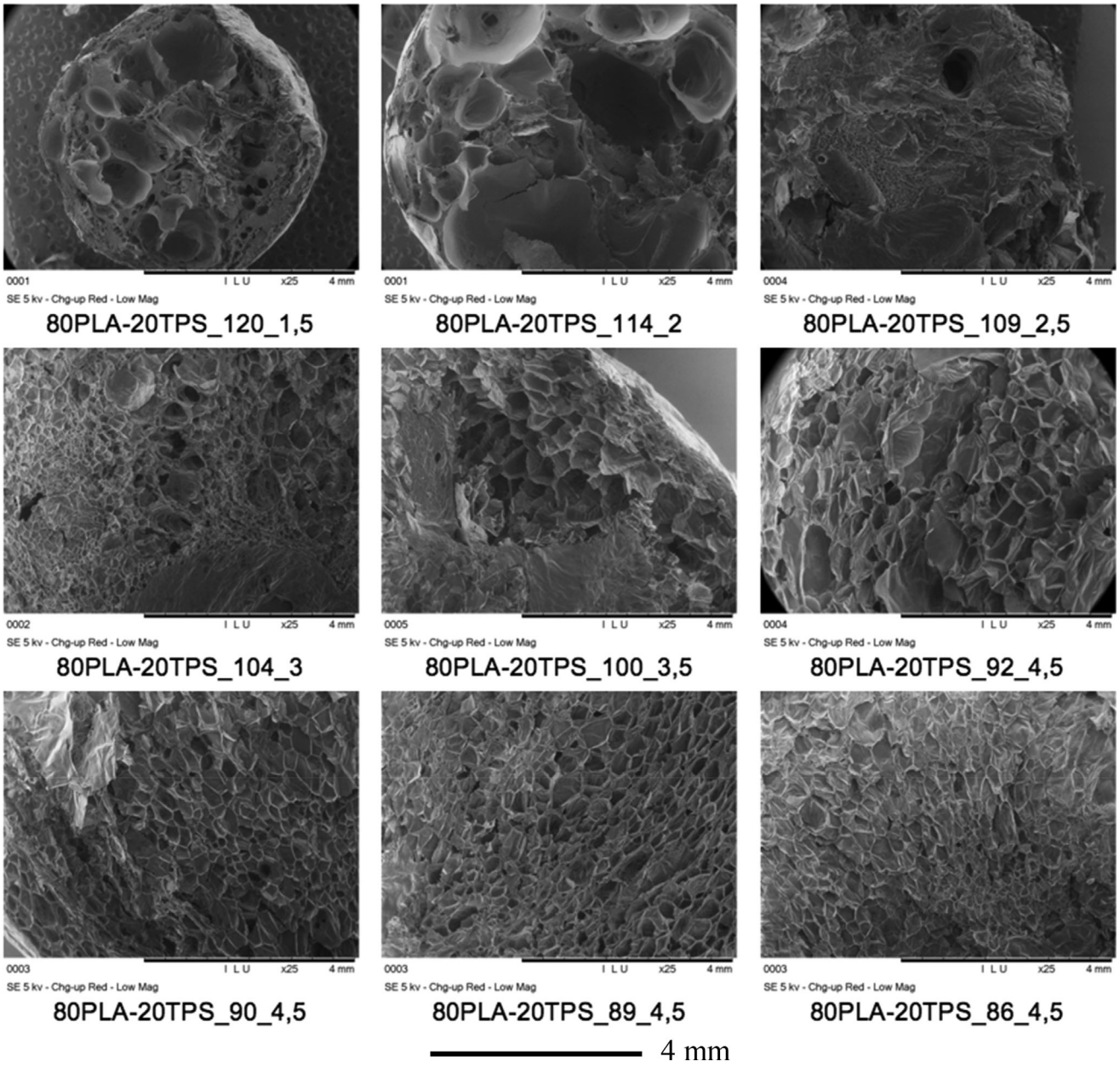

FIGURE 4 SEM microphotographs of 80PLA/20TPS foams at different die temperatures

3.1.2 | Blend of 50PLA/50TPS

For the blend of 50PLA/50TPS, Figure 3 confirms the well-known weak affinity between PLA and TPS when no compatibilizer is added. The structure of the foams was coarser than for TPS alone with large craters. The foam structure was open and torn for all samples. These images suggest that it could be useful to add a coupling agent to improve the interface between the two polymers. By looking the microphotography, it could be anticipated that mechanical foam properties will be weak.

3.1.3 | Blend of 80PLA/20TPS

The best structures were obtained for the blend consisting of 80PLA/20TPS as illustrated in Figure 4. With die temperature reduction, cell size seems to diminish and the nucleation was greater. Cell walls appeared not broken. However, this figure shows the lack of affinity between both polymers because large unfoamed areas were visible. By comparing with Figure 2, it is likely that these areas were made of TPS alone. Cell distribution remained inhomogeneous. Similar results were obtained by Mihai et al.[20] They suggested to use a compatibilizer, PLA grafted with maleic anhydride (PLA-g-MA), for getting a better interface and affinity between PLA and TPS.

3.2 | Expansion and porosity

The total porosity and the total expansion as a function of the die temperature have been plotted in Figure 5. The effect of die temperature was different depending on the blend composition.

For pure TPS, a foam of 70% porosity was created upon CO_2 injection. With the lowering of die temperature, a slight increase in the porosity was observed but stayed below 80%.

To explain this rather low porosity, two hypotheses can be made. First, about the filling of the extruder: extrusion foaming was very difficult for pure TPS possibly due to the presence of excess CO_2 in the barrel. Rizvi and Mulvaney[25] have explained in their patent, the importance of a good filling of the extruder barrel to avoid the formation of two different phases between the starch and the CO_2, leading in turn to poor porosity. Second, low melt strength combined to very low Tg of the TPS (−45°C) could not prevent CO_2 from escaping outside the polymer matrix giving open porosity and relatively low global expansion. It could be observed that the expansion efficiency was low for 50PLA/50TPS, confirming a large escape of CO_2 from the melt before foaming (Figure 6).

The blend consisting in 80% PLA with 20% TPS displayed a different behavior. Just after the CO_2 injection, only 25% porosity was created. However, with the die temperature diminution, the porosity raised until reaching a maximum of 96%. In this case, the expansion efficiency increased up to almost 50%, confirming a better use of CO_2 as blowing agent (Figure 6). Below 96°C, the porosity slightly lessened to 94% correlatively to the PLA melt strength increase. Lower graph of Figure 5, showing the total expansion, highlights the result obtained for the total porosity. These results were very promising, because in spite of the lack of affinity between both polymers as illustrated in SEM images, porosity as high as 96% could be obtained.

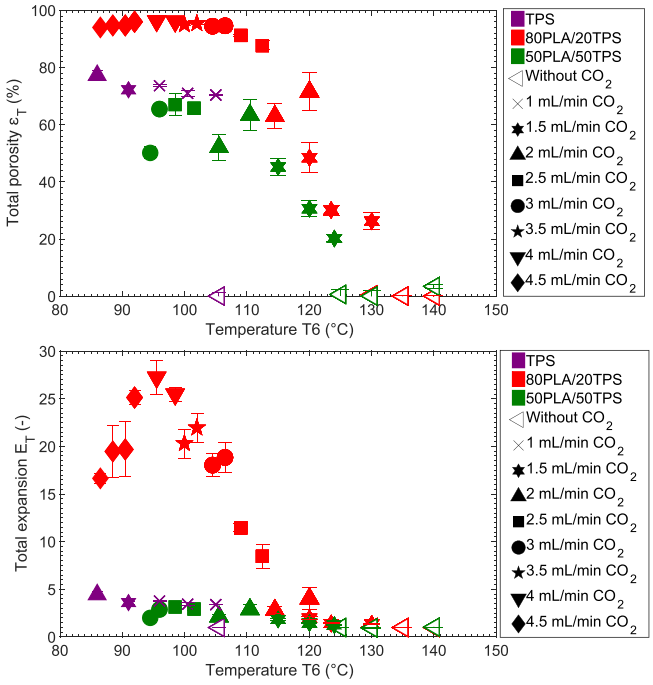

FIGURE 5 Total porosity and expansion as a function of die temperature T_6 [Color figure can be viewed at wileyonlinelibrary.com]

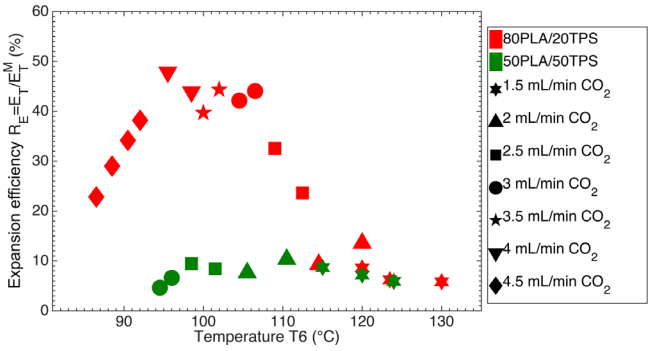

FIGURE 6 Expansion efficiency R_E as a function of die temperature T_6 [Color figure can be viewed at wileyonlinelibrary.com]

By comparing the result obtained for pure PLA by Chauvet et al.[12] and the blend of 80PLA/20TPS, the main difference is the threshold temperature associated with the diminution of porosity. For pure PLA, the threshold temperature was 109°C, here, the die temperature was below 95°C. The incorporation of TPS in PLA probably changed the rheological properties, in particularly the melt strength. The pressure in the die was lower for the blend than for the PLA alone,[12] indicating a less viscous melt.

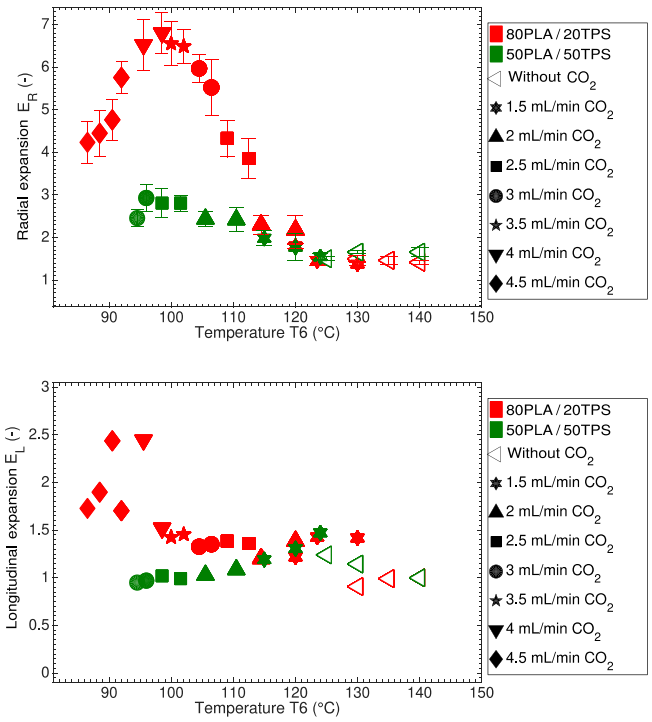

FIGURE 7 Radial and longitudinal expansion of the foams as a function of the temperature T_6 [Color figure can be viewed at wileyonlinelibrary.com]

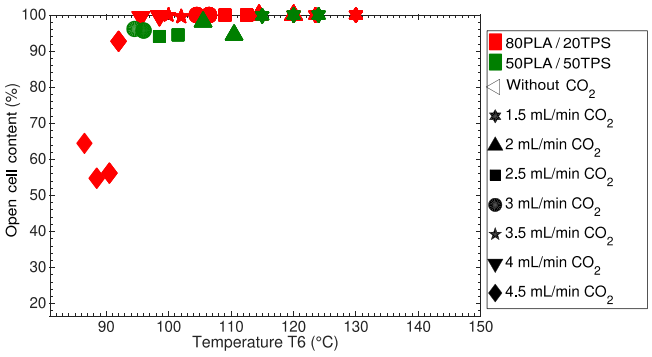

FIGURE 8 Open cell content of the foams as a function of temperature T_6 [Color figure can be viewed at wileyonlinelibrary.com]

In comparison, Mihai et al.[20] have obtained a foam with a density of 34 kg/m^3 and porosity of 97% for a blend of 67% PLA and 33% TPS. When the authors added PLA-g-MA to their blend, density decreased to 25 kg/m^3, corresponding to a porosity of 98%. These results indicated that PLA-g-MA had little influence on the porosity for a composition of 67% PLA and 33% TPS.

The 50PLA/50TPS blend showed an intermediate behavior. With the die temperature diminution, porosity increased from 20% to 70% with the addition of CO_2, indicating a behavior similar to that of pure PLA. However, when die temperature was kept below 110°C, the foam behaved like pure TPS: porosity stayed at approximately 65% as displayed by the bottom graph of Figure 5. Poor interfacial adhesion between both biopolymers at this content of 50/50 was evidenced as confirmed by the SEM images.

In comparison Mihai et al.[20] have obtained a foam with a density of 624 kg/m^3 without PLA-g-MA (50% porosity) but with the coupling agent, they obtained a density of 71 kg/m^3 (95% porosity). They explained the low porosity for the blend without any coupling agent by the presence of large TPS unfoamed areas.

3.3 | Foam structure

A maximum of the radial expansion was observed for the higher expansion, while the longitudinal expansion increased significantly (for 80PLA/20TPS) below the critical temperature of higher expansion (Figure 7). It clearly indicated the same change of phenomenology as previously observed for pure PLA by Chauvet et al.[12] The increasing polymer stiffness at low temperature led to a "frozen" surface of the extrudate preventing the gas to escape from this melt and resulting in a longitudinal expansion. As previously observed,[12] this phenomenology

TABLE 5 Parameters determined by MDSC analysis

	Reversible HF		Non-reversible HF		Total HF		
Sample	**T_g (°C)**	**ΔCp (J g^{-1} °C^{-1})**	**T_{cc} (°C)**	**ΔH_{cc} (J/g)**	**T_m (°C)**	**ΔH_m (J/g)**	**χ (%)**
80PLA/20TPS_104_3	57.6	0.4	82.9	19	143.2	22.6	4.8
80PLA/20TPS_86_4.5	57.5	0.4	75.5	15	141.1	23.8	11.7
50PLA/50TPS_96_3	57;2	0.2	75.8	9.1	137.7	13.1	8.7

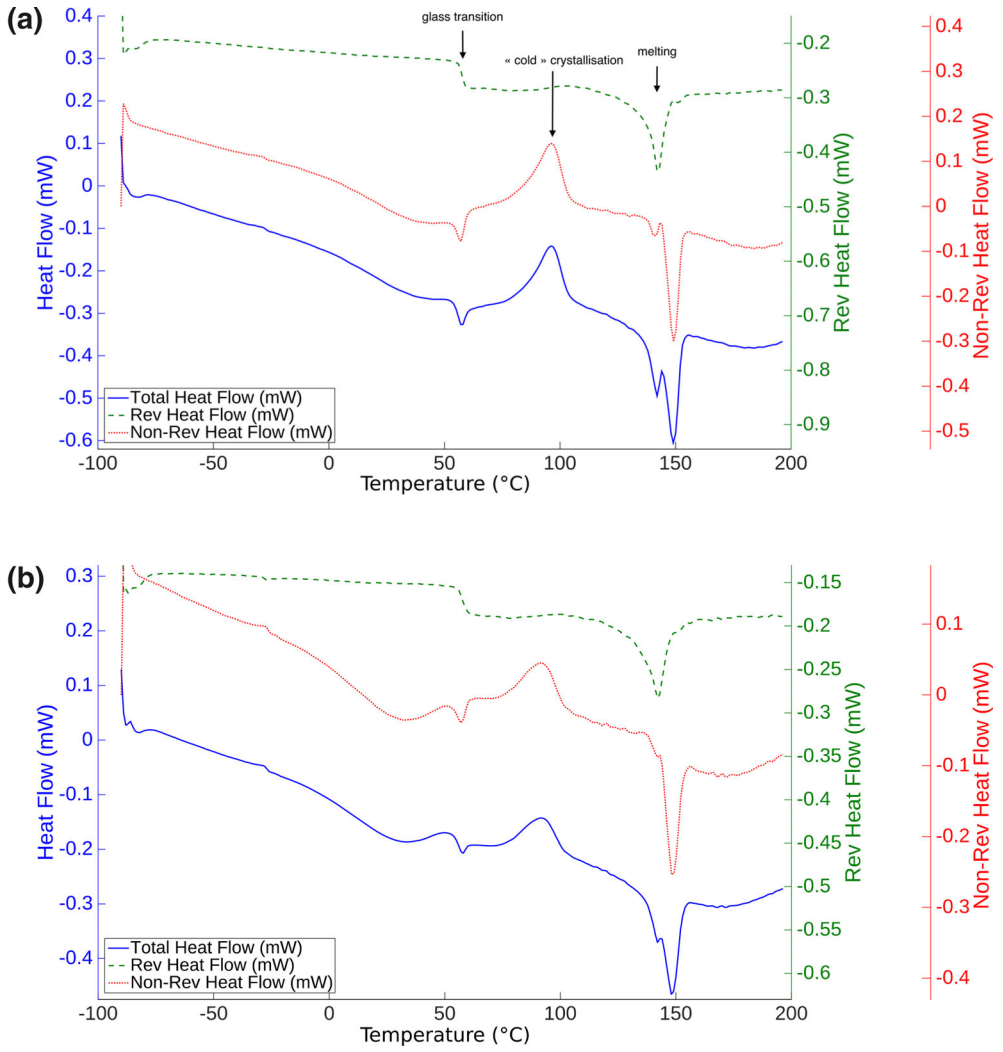

FIGURE 9 MDSC curves of 80PLA/20TPS blend. (a) Sample 80PLA/20TPS_104_3, (b) sample 80PLA/20TPS_86_4.5 [Color figure can be viewed at wileyonlinelibrary.com]

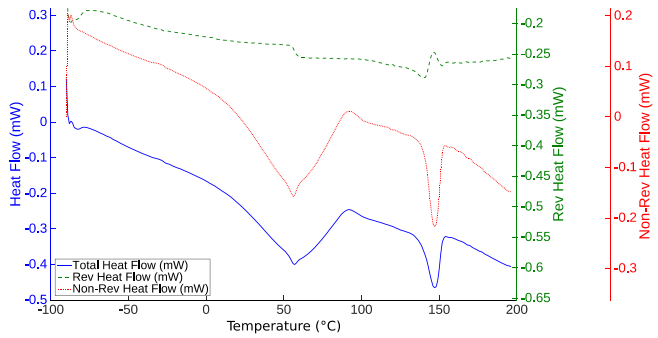

FIGURE 10 MDSC curves of sample 50PLA/50TPS_96_3 [Color figure can be viewed at wileyonlinelibrary.com]

change was associated to the formation of closed porosity at temperatures lower than the critical one, whereas there was only open porosity at higher temperatures (Figure 8).

3.4 | Thermal analysis and crystallinity

Table 5 shows the MDSC parameters of two 80PLA/20TPS samples, and one 50PLA/50TPS sample, the graphs of which are presented in Figures 9 and 10.

3.4.1 | MDSC curves of 80PLA/20TPS blend

The curves presented in Figure 9 had been made with two samples 80PLA/20TPS_104_3 (Figure 9(a)) and 80PLA/20TPS_86_4.5 (Figure 9(b)), representing 2 die temperatures.

Glass transition: the glass transition temperature of PLA had been slightly affected by the addition of TPS: 57°C (vs. 59°C for pure PLA). This small decrease in the glass transition temperature thus indicated a partial miscibility of the two biopolymers.

At −20°C, a slight endothermic peak was present in both graphs. This event was attributed to TPS because it was also present on the MDSC curve of pure TPS (data not shown).

Cold crystallization: the exothermic peak of cold crystallization of PLA was clearly observable. For samples made between 104 and 140°C, the peak was narrow (see Figure 9(a)) with a ΔH_{cc} of 19 J/g, it started around 85°C. This cold crystallization temperature was lower than that of pure PLA. Teixeira et al.[26] found similar results: a decrease in cold crystallization temperature with the addition of TPS, the higher the TPS content, the larger the temperature drop. The addition of TPS might have a nucleation effect on the PLA crystallization. For samples manufactured between 86 and 99°C (Figure 9(b)), a broader crystallization peak with a smaller enthalpy (15 J/g) could be seen. For these samples, cold crystallization began around 75°C. This temperature was similar to that of pure PLA extruded at low temperature and indicated a change in the kinetics of crystallization which was related to shearing in the extruder.

Melting: the last visible event on the MDSC signals was the melting represented by an endothermic peak. Two melting peaks appeared for samples manufactured between 104 and 14°C, at a temperature of 144°C. For samples made at low temperatures, the melting temperature was slightly lower (141°C) and the first peak had become a shoulder.

In conclusion, the 80PLA/20TPS blend behaved globally like pure PLA[12]: extruded at low temperature, a drop in the crystallization and melting temperature were observable. In addition, these phenomena occurred at a lower die temperature than for pure PLA.

3.4.2 | MDSC graphs of 50PLA/50TPS blend

A MDSC curve for a 50PLA/50TPS sample is shown in Figure 10.

Glass transition: it occurred around 56°C. As for the previous blend, this decrease in Tg (in comparison to pure PLA) indicated a partial miscibility between the two polymers. As mentioned for the previous blend, an endotherm at −20°C was also visible for this 50PLA/50TPS blend.

Cold crystallization: this peak was strongly affected by the incorporation of TPS. On the non-reversible heat flow signal, the cold crystallization took place while the enthalpy relaxation was not finished. This led to a broad exothermic peak, without a clear baseline, making difficult a proper integration. Exothermic peaks showed an enthalpy of 11 J/g for samples made between 115 and 140°C, while for lower die temperatures the enthalpy was smaller (8 J/g). The incorporation of TPS in the PLA matrix, could have hindered the PLA chain organization and thus have modified the kinetics of crystallization.

Melting: For extruded samples at a die temperature of 124–140°C, the melting temperature was 142°C, while for lower die temperatures the melt temperature was shifted to lower temperature (138°C). With the decrease of the die temperature the second melting peak tended to disappear.

In conclusion, the addition of 50% TPS significantly changed the behavior of the PLA.

3.4.3 | Crystallinity

The crystallinities of the samples calculated using Equation (6), are given in Tables 3 and 4.

For the 80PLA/20TPS blend: the behavior with the evolution of die temperature was similar to that of pure PLA. An increase in crystallinity was observed when T_6 decreased. More particularly, for samples made below 92°C, the crystallinity was close to 11%. Samples with such a high crystallinity showed a different behavior. They exhibited lower porosity and expansion rate and a close-type porosity. This went with a high pressure upstream the die during the tests (10 MPa). These three parameters indicated an increase in melt strength due to the nucleated crystal lattice.

The addition of TPS lowered the crystallinity level of PLA from 15% to 11%. In contrast, Li and Huneault[27] and Mihai et al.[20] observed an increase in the crystallinity of PLA with the addition of TPS and explained this increase by the presence of a coupling agent (PLA-g-MA), which made possible a size reduction of the TPS particles. No agent of this type has been used in our study and the poor miscibility between the polymers prevented the enhancement of nucleation to occur.

For the 50PLA/50TPS blend, the crystallinity level values were more difficult to elucidate. The degree of crystallinity varied between 3% and 16%. It raised with the decrease of the die temperature. Unlike the previous mixture, no change in porosity or type of porosity with increasing crystallinity could be observed. This was attributed to the incompatibility between the two polymers which became predominant at this TPS content.

4 | CONCLUSIONS

Foams of biopolymer blends (PLA and TPS) were successfully manufactured by hot-melt extrusion with supercritical CO_2 as a blowing agent. The two tested blends exhibited however different behavior.

The blend of 80% PLA and 20% TPS gave similar results for all the properties measured in comparison to pure PLA. Porosity levels as high as 96% have been obtained and a threshold die temperature separating a close cell porosity (at lowest temperatures) and an open cell structure (above the threshold) could be observed. This temperature threshold was however significantly lowered to 95°C instead of 109°C with pure PLA. This is due to the incorporation of TPS in PLA, which has changed the rheological properties, particularly the melt strength. The porous structure was still regular, but zones of poor foaming have started to appear.

On the other hand, the blend made of 50% PLA and 50% TPS displayed discrepancies due to the strong incompatibility between the two biopolymers, confirmed by a lower porosity and a very coarse pore structure. Indeed, TPS is amorphous, with a low glass transition temperature (−45°C) and its addition favored the gas escape from the sample at the die exit. Adding a greater proportion of TPS in the blend would require the addition of an agent able to improve the affinity between the two polymers. This hypothesis is currently under investigation.

ACKNOWLEDGMENTS

Authors gratefully acknowledge the financial support of the *Région Occitanie* in form of a doctoral scholarship to the first author. They also thank the technical team of the RAPSODEE research centre: Sylvie Del Confetto for the MDSC analysis and Christine Rolland for the SEM images.

Part of this work was presented at the 16th European Meeting on Supercritical Fluids held in Lisbon, Portugal on April 2017.

ORCID

Martial Sauceau https://orcid.org/0000-0002-2709-1016
Fabien Baillon https://orcid.org/0000-0003-0649-9386
Jacques Fages https://orcid.org/0000-0001-9280-9007

REFERENCES

[1] S. J. Huang, *J. Macromol. Sci. Part A* **1995**, *32*, 593.
[2] M. Chauvet, M. Sauceau, J. Fages, *J. Supercrit. Fluids* **2017**, *120*, 408.
[3] R. Auras, B. Harte, S. Selke, R. Hernandez, *J. Plast. Film Sheeting* **2003**, *19*, 123.
[4] R. Auras, B. Harte, S. Selke, *Macromolecular Bioscience* **2004**, *4*, 835. http://dx.doi.org/10.1002/mabi.200400043.
[5] D. R. Lu, C. M. Xiao, S. Xu, *J. Express Polym. Lett.* **2009**, *3*, 366.
[6] Y. Zhang, C. Rempel, Q. Liu, *Crit. Rev. Food Sci. Nutr.* **2014**, *54*, 1353.
[7] E. Di Maio, E. Kiran, *J. Supercrit. Fluids* **2018**, *134*, 157.
[8] J. A. Villamil Jiménez, N. Le Moigne, J.-C. Bénézet, M. Sauceau, R. Sescousse, J. Fages, *Molecules* **2020**, *25*, 3408. http://dx.doi.org/10.3390/molecules25153408.
[9] C. Nikitine, E. Rodier, M. Sauceau, J. J. Letourneau, J. Fages, *J Appl Polym Sci* **2010**, *115*, 981. http://dx.doi.org/10.1002/app.31031.
[10] N. Le Moigne, M. Sauceau, M. Benyakhlef, R. Jemai, J.-C. Benezet, E. Rodier, J.-M. Lopez-Cuesta, J. Fages, *Eur. Polym. J.* **2014**, *61*, 157. http://dx.doi.org/10.1016/j.eurpolymj.2014.10.008.
[11] K. Bocz, T. Tabi, D. Vadas, M. Sauceau, J. Fages, Gy. Marosi, *Express Polym. Lett.* **2016**, *10*, 771. http://dx.doi.org/10.3144/expresspolymlett.2016.71.
[12] M. Chauvet, M. Sauceau, F. Baillon, J. Fages, *J Appl Polym Sci* **2017**, *134*, 45067. http://dx.doi.org/10.1002/app.45067.
[13] S. Jacobsen, H. G. Fritz, *Polym. Eng. Sci.* **2799**, *1996*, 3.
[14] J. W. Park, S. S. Im, S. H. Kim, Y. H. Kim, *Polym. Eng. Sci.* **2539**, *2000*, 40.
[15] W. Ning, Y. Jiugao, M. Xiaofei, *Polym. Compos.* **2008**, *29*, 551.
[16] A. S. Walallavita, C. J. R. Verbeek, M. C. Lay, *J Appl Polym Sci* **2017**, *134*, 45561.
[17] M. A. Huneault, H. Li, *Polymer (Guildf)* **2007**, *48*, 270.
[18] O. H. Arroyo, M. A. Huneault, B. D. Favis, M. N. Bureau, *Polym. Compos.* **2010**, *31*, 114.
[19] R. Iovino, R. Zullo, M. A. Rao, L. Cassar, L. Gianfreda, *Polym. Degrad. Stab.* **2008**, *93*, 147.
[20] M. Mihai, M. A. Huneault, B. D. Favis, H. Li, *Macromol. Biosci.* **2007**, *7*, 907.
[21] Carbon dioxide, NIST Chemistry WebBook, http://webbook.nist.gov/cgi/cbook.cgi?ID=124-38-9.
[22] C. B. Park, A. H. Behravesh, R. D. Venter, *Polym. Eng. Sci.* **1998**, *38*, 1812.
[23] J. Wang, W. Zhu, H. Zhang, C. B. Park, *Chem. Eng. Sci.* **2012**, *75*, 390.
[24] E. W. Fischer, H. J. Sterzel, G. Wegner, *Kolloid-Z. Z. Polym.* **1973**, *251*, 980.
[25] S. S. H. Rizvi; S. J. Mulvaney Extrusion processing with supercritical fluids. US Pat 5,120,559 1992.
[26] E. de Morais Teixeira, A. A. S. Curvelo, A. C. Corrêa, J. M. Marconcini, G. M. Glenn, L. H. C. Mattoso, *Ind. Crops. Prod.* **2012**, *37*, 61.
[27] H. Li, M. A. Huneault, *Int. Polym. Process.* **2008**, *23*, 412.